Polymer 51 (2010) 2533–2539

Contents lists available at ScienceDirect

Polymer

journal homepage: www.elsevier.com/locate/polymer

Preparation of magnetite and tumor dual-targeting hollow polymer microspheres with pH-sensitivity for anticancer drug-carriers

Xiaoying Yang [a,*], Lei Chen [a], Bin Han [a], Xinlin Yang [b,**], Hongquan Duan [a]

[a] School of Pharmaceutical Sciences, Basic Medical Research Center, Tianjin Medical University, Tianjin 300070, China
[b] Key Laboratory of Functional Polymer Materials, Ministry of Education, Institute of Polymer Chemistry, Nankai University, Tianjin 300071, China

ARTICLE INFO

Article history:
Received 23 December 2009
Received in revised form
7 April 2010
Accepted 16 April 2010
Available online 22 April 2010

Keywords:
Distillation precipitation polymerization
Magnetite and tumor dual-targeting
pH-Sensitivity

ABSTRACT

The hollow poly(*N,N′*-methylenebisacrylamide-*co*-methacrylic acid) (P(MBAAm-*co*-MAA)) microspheres were prepared by the selective removal of poly(methacrylic acid) (PMAA) core from the corresponding PMAA/P(MBAAm-*co*-MAA) core-shell microspheres, which were synthesized via a two-stage distillation precipitation polymerization. The magnetic Fe_3O_4 nanoparticles onto the surface of hollow P(MBAAm-*co*-MAA) microspheres via partial oxidation of ferrous salt during the chemical deposition in the presence of potassium nitrate as oxidant with the aid of hexamethylene tetramine and the magnetic hollow microspheres were further functionalized with folic acid (FA) via the chemical linkage with amino groups of 3-aminopropyl triethoxysilane (APS)-modified P(MBAAm-*co*-MAA)@Fe_3O_4 microspheres to afford the magnetite and tumor dual-targeting hollow microspheres. The resultant dual-targeting hollow polymer microspheres with pH-sensitivity were characterized by transmission electron microscopy (TEM), dynamic light scattering (DLS), Fourier transform infrared-spectrometer (FT-IR), UV–vis absorption spectroscopy, and vibrating sample magnetometer (VSM). Finally, the drug loading capacities of the magnetite and tumor dual-targeting hollow P(MBAAm-*co*-MAA) microspheres and their releasing dependence on pH values were investigated with doxorubicin hydrochloride (DXR) as an anticancer drug model.

1. Introduction

During the last decade, hollow polymer microspheres have attracted increasing attention due to their wide applications, such as encapsulation for controlled release of drugs and enzymes, fillers, pigments, catalysts, and adsorption materials for sound [1–4]. Significant progress has been made for the design and synthesis of hollow polymer particles by a variety of physical and chemical techniques [5–9]. Among them, environmentally responsive polymer capsules and polymer microspheres, including pH-sensitive [9–11], thermo-sensitive [12,13], iron-strength [14], magnetism [15], and dual thermo-responsive and ion-recognizable [16], have been prepared by different methods for various applications, such as for practical utilization in controlled release [12]. In such a context, the synthesis of hollow polymer microspheres with stimuli sensitivity and narrow size distribution warrants further exploration, which will be of both scientific and technical interest.

Magnetic particles, for example, magnetite (Fe_3O_4) nanoparticles have various applications, such as magnetic storage media, printing inks, magnetic resonance imaging, drug delivery, biomedicine, biosensors, magnetic separation, ferro-fluid, and catalysis [17–21] due to their extraordinary magnetic, optical, and biocompatible properties. However, these nano-sized magnetite particles tend to aggregate because of their high specific area and strong interparticle interaction, which limit their utilization. Therefore, it is necessary to develop strategies for the chemical stabilization of the naked magnetic nanoparticles against aggregation over a long period. The formation of magnetite/polymer hybrid/composite materials not only stabilized the magnetic nanoparticles, but also endowed the magnetic nanoparticles with functionality. In such a way, magnetic/polymer microspheres have found wide applications in the fields of biology, medicine, catalysis and many other areas [22–26]. The preparation of magnetite/polymer particles can be afforded via generally three categories, which included physical or physicochemical interaction between the pre-formed magnetic particles and polymer particles [27,28], *in-situ* precipitation of iron-oxides in the presence of polymer microspheres [29] and *in-situ* polymerization of monomers in the

* Corresponding author. Tel.: +86 22 23542803; fax: +86 22 23503510.
** Corresponding author. Tel.: +86 22 23502023; fax: +86 22 23503510.
E-mail addresses: yangxiaoying@tijmu.edu.cn (X. Yang), xlyang88@nankai.edu.cn (X. Yang).

0032-3861/$ – see front matter © 2010 Elsevier Ltd. All rights reserved.
doi:10.1016/j.polymer.2010.04.032

presence of magnetic nanoparticles [30–35]. However, it was difficult to control the distribution of the magnetic nanoparticles in the magnetite/polymer composites for emulsion polymerization [23] and the morphology of the resultant composite particles via a sol–gel process [36].

Folic acid (FA) has been used widely as targeting molecule for the targeted delivery of therapeutic molecules [37] because it can bind to a tumor-associated antigen known as the folate receptor (FR), which is generally over-expressed in several types of human cancers, especially leukemic cells [38] and ovarian tumor [39]. An ideal delivery carrier for an anticancer drug should be able to transport the drugs specifically to cancer cells and release the drug molecules inside the cells. Since the drug-loaded carriers are taken up to the tumor cell interior through endocytosis, then endocytic carriers change from early and late endosomes and finally to lysosomes in which the proton concentration (pH 5.0) is 100-times higher than the physiological condition (pH 7.4). Therefore, the pH-sensitivity is an important *in vivo* chemical stimuli for the effective release of anti-tumor drug in tumor cells [40,41].

In order to enhance the effect of targeted delivery, a dual-targeting delivery system was established for drug delivery with doxorubicin hydrochloride (DXR) as a model molecule. The magnetite and tumor dual-targeting hollow polymer microspheres were originated from the targeted delivery based on the forces of a magnetic field and the specific interaction between the folic acid on the drug-carriers and the over-expressed folate receptor on the surface of some tumor cells. In our previous works, the loading and controlled-release behavior of the drugs on the hollow thermo-responsive poly(*N*-isopropylacrylamide) (PNIPAAm) [13] and pH-sensitive poly(*N,N′*-methylenebisacrylamide-*co*-methacrylic acid) (P(MBAAm-*co*-MAA)) [42] microspheres were investigated with DXR as a model drug. Herein, we reported the design and synthesis of monodisperse hollow magnetite and tumor dual-targeting P(MBAAm-*co*-MAA) microspheres with pH-sensitivity as an approach to enhance targeting selectivity of drug selectivity of drug-loaded carriers for avoiding the serious side-effects from the non-specific uptake of the drugs. Further, the drug loaded in such magnetite and tumor dual-targeting hollow polymer microspheres were well controlled release via the pH values in the environment.

2. Experimental

2.1. Chemicals

N, N′-Methylenebisacrylamide (MBAAm, chemical grade, Tianjin Bodi Chemical Engineering Co.) was recrystallized from acetone. Methacrylic acid (MAA) was got from Tianjin Chemical Reagent II Co. and was purified by vacuum distillation. 2,2′-Azobisisobutyronitrile (AIBN, analytical grade) was available from Chemical Factory of Nankai University and recrystallized from methanol. Acetonitrile (analytical grade, Tianjin Chemical Reagents II Co.) was dried over 4 Å molecular sieves and purified by distillation. Ferrous chloride tetrahydrate ($FeCl_2 \cdot 4H_2O$), hexamethylene tetramine (HETM) and sodium hydroxide were purchased from Tianjin No. 3 Chemical Plant. 3-Aminopropyl trimethoxysilane (APS) was purchased from Aldrich and used without further purification. Folic acid (FA) was bought from Nanjing Boquan Technology Co. and used as received. 1-Ethyl-3-(3-dimethylaminopropyl)carbodiimide (EDC) was purchased from Aldrich. Doxorubicin hydrochloride (DXR) was provided by Beijing Huafeng United Technology Co. and used without further purification. All the other reagents were analytical grade and used without any further treatment.

2.2. Preparation of monodisperse hollow P(MBAAm-co-MAA) microspheres

Monodisperse polymethacrylic acid (PMAA) microspheres were prepared according to the procedure in our previous work by distillation precipitation polymerization in acetonitrile with AIBN as initiator in the absence of any crosslinker or stabilizer [42], which was considered as the first-stage polymerization in the present work. A typical procedure for such polymerization was as follows: MAA (4 mL, 4 g, 46.6 mmol), AIBN (0.08 g, 0.48 mmol, 2 wt% relative to the monomer) were dissolved in 160 mL of acetonitrile in a dried 250 mL two-necked flask attaching with a fractionating column, Liebig condenser, and a receiver. The flask was submerged in a heating mantle, and the reaction mixture was heated from ambient temperature till boiling state within 15 min, and then the solvent was distilled from the reaction system. The reaction mixture became milky white after boiling for 10 min. The reaction was ended after 80 mL of acetonitrile was distilled from the reaction system within 2 h. After the polymerization, the resultant PMAA microspheres were purified by repeating centrifugation, decanting, and resuspension in acetonitrile with ultrasonic bathing for three times.

Monodisperse PMAA/poly(*N,N′*-methylenebisacrylamide-*co*-methacrylic acid) (PMAA/P(MBAAm-*co*-MAA)) core-shell microspheres were synthesized by the second-stage distillation precipitation polymerization of MAA and MBAAm in the presence of PMAA microspheres as seeds with AIBN as initiator in acetonitrile. In a typical experiment, PMAA seeds (0.70 g), 0.10 g MBAAm crosslinker, 0.40 mL (0.40 g) of MAA comonomer and 0.01 g of AIBN (2 wt % of the total comonomers) were added in 80 mL of acetonitrile at room temperature in a 100-mL of two-necked flask equipping with a fractionating column, a Liebig condenser, and a receiver. The flask was submerged in a heating mantle and the second-stage polymerization mixture was heated from the ambient temperature to the boiling state within 15 min. Then the solvent (40 mL of acetonitrile) was distilled off the reaction system within 70 min. After the polymerization, the resultant PMAA/P(MBAAm-*co*-MAA) core-shell microspheres were purified by ultracentrifugation, decantation and washing with acetonitrile for three times.

The PMAA/P(MBAAm-*co*-MAA) core-shell microspheres were dispersed in ethanol with stirring for 1–2 days and the non-crosslinked PMAA core were selectively dissolved in ethanol. The corresponding hollow P(MBAAm-*co*-MAA) microspheres were obtained by washing with ethanol and centrifugation and then by further washing with ethanol and centrifugation for three times to remove the residual PMAA components on the surface of hollow polymer microspheres.

2.3. Preparation of magnetic P(MBAAm-co-MAA)@Fe_3O_4 hollow microspheres

$FeCl_2 \cdot 4H_2O$ (0.30 g) and KNO_3 (0.05 g) were mixed in 75 mL of ethyleneglycol (EG) aqueous solution (EG/water = 15/60 mL) in the presence of hollow P(MBAAm-*co*-MAA) microspheres (0.08 g) and HETM (1.0 g). The resulting hollow P(MBAAm-*co*-MAA) microspheres were heated at 80 °C for 3 h under nitrogen to obtain magnetite nanoparticles-loaded P(MBAAm-*co*-MAA)@Fe_3O_4 hollow microspheres. After cooling to room temperature, the magnetic P(MBAAm-*co*-MAA)@Fe_3O_4 hollow microspheres were centrifugated and washed with distilled water.

2.4. Magnetic P(MBAAm-co-MAA)@Fe_3O_4 hollow microspheres conjugating with folic acid

The afforded P(MBAAm-*co*-MAA)@Fe_3O_4 hollow microspheres were dispersed in 3.0 mL of APS in 200 mL of ethanol aqueous

solution (water/ethanol = 40/160 mL). The suspension was ultrasonicated and stirred for 48 h at room temperature. Then the suspension was centrifugated and the precipitates were washed with distilled water. The APS-modified magnetic P(MBAAm-*co*-MAA)@Fe_3O_4 hollow microspheres were obtained.

FA (0.35 g) and EDC (0.15 g) were dissolved in 30 mL of DMF and ultrasonicated for 1 h. The mixture was ultracentrifugated and supernatant was stored for the following reaction. Then the above APS-modified magnetic P(MBAAm-*co*-MAA)@Fe_3O_4 hollow microspheres were added into the supernatant and stirred for 12 h at room temperature. After the conjugating reaction, the suspension was ultracentrifugated and the precipitates were washed with distilled water to afford magnetite and tumor dual-targeting P (MBAAm-*co*-MAA) hollow microspheres.

2.5. Drug loading and release behavior of the magnetite and tumor dual-targeting P(MBAAm-co-MAA) hollow microspheres

A series of DXR solutions with different initial concentrations were mixed with respect to the same concentration of hollow magnetite and tumor dual-targeting P(MBAAm-*co*-MAA) hollow microspheres (0.40 mg/mL). The loading of the drug took place in the suspension on an SHA-B shaker with gentle agitation by rolling the bottles in a horizontal position to approximately 40 rpm for 24 h. The unloaded DXR molecules were removed from the system by ultracentrifugation. The loading capacity of DXR on the dual-targeting P(MBAAm-*co*-MAA) hollow microspheres was determined by ultraviolet–visible (UV–vis) spectra with irradiation source at wavelength of 480 nm, which was calculated by the difference of DXR concentration between the original DXR solution and the supernatant after loading process and the DXR concentration was calibrated from a standard curve of DXR aqueous solution. During this operation, the supernatant after ultracentrifugation in the presence of dual-targeting P (MBAAm-*co*-MAA) hollow microspheres without DXR was processed under the same conditions as a blank sample for determination.

The dual-targeting P(MBAAm-*co*-MAA) hollow microspheres (12.0 mg) loaded with DXR under the neutral conditions were dispersed in 4.0 mL of aqueous solution and the suspension was divided into four aliquots. The drug-loaded dual-targeting P (MBAAm-*co*-MAA) hollow microspheres used for the release determination were placed into the dialysis chambers, which were dialyzed in 80 mL of aqueous solution under different pH environments, such as pH = 7.4, 6.0, 5.0 and 4.0, respectively. The drug release was assumed to start as soon as the dialysis chambers were placed into the reservoir. The release reservoir was kept under constant stirring, and one of the dialysis chambers was taken out for characterization at various time points. The concentration of DXR released from dual-targeting P(MBAAm-*co*-MAA) hollow microspheres into aqueous solution was quantitatively analyzed by UV–vis spectroscopy with irradiation wavelength number of 480 nm.

2.6. Characterization

The morphology of the resultant polymer microspheres was determined by transmission electron microscopy (TEM) using a Technai G2 20-S-TWIN microscope. Samples for TEM characterization were dispersed in a solvent and a drop of the dispersion was spread onto the surface of a copper grid coated with a carbon membrane. The size and size distribution reflect the average of about 100 particles, which are calculated according to the following formula:

$$U = D_w/D_n,\ D_n = \sum_{i=1}^{k} n_i D_i / \sum_{i=1}^{k} n_i,\ D_w = \sum_{i=1}^{k} n_i D_i^4 / \sum_{i=1}^{k} n_i D_i^3$$

where U is the polydispersity index, D_n is the number-average diameter, D_w is the weight-average diameter, D_i is the particle diameter of the determined microparticles.

The average particle size and size distribution of the magnetic P (MBAAm-*co*-MAA)@Fe_3O_4 hollow microspheres were measured in ethanol by a Zeta Potential Analyzer (Brookhaven Instruments Corporation, USA) equipped with Size Analyzer with 90 Plus at 659 nm.

Fourier transform infrared spectra (FT-IR) were determined on a Bruker Tensor 27 FT-IR spectrometer over potassium bromide pellet and the diffuse reflectance spectra were scanned over the range of 400–4000 cm^{-1}.

The magnetization curve of the magnetic P(MBAAm-*co*-MAA) @Fe_3O_4 hollow microspheres was measured as a function of applied magnetic field H with a 9600 VSM (LDJ Co., USA) superconducting quantum interference device (SQUID) magnetometer. The hysteresis of the magnetization was obtained by varying H between +6000 and −6000 Oe at 300 K.

UV–vis absorption spectra were scanned on a JASCO V-570 ultraviolet–visible-near-IR spectrometer (UV–vis–NIR) and the loading capacity of the magnetite and tumor dual-targeting P (MBAAm-*co*-MAA) hollow microspheres toward DXR were determined with a laser source of wavelength at 480 nm as an excitation source for the determination of the concentration for DXR.

3. Results and discussion

Scheme 1 illustrated the preparation of the magnetite and tumor dual-targeting P(MBAAm-*co*-MAA) hollow microspheres, their application for anticancer drug-carriers, and the chemical structures of FA and DXR, respectively. At first, the hollow P (MBAAm-*co*-MAA) microspheres were prepared by the selective removal of non-crosslinked PMAA core from the corresponding PMAA/P(MBAAm-*co*-MAA) core-shell microspheres, which were synthesized by a two-stage distillation precipitation polymerization. Then the magnetite and tumor dual-targeting P(MBAAm-*co*-MAA) hollow microspheres were synthesized via loading Fe_3O_4 nanoparticles onto P(MBAAm-*co*-MAA) hollow microspheres with the subsequent conjugation of FA via amide linkage with amino group of APS-modified the magnetic hollow P (MBAAm-*co*-MAA)@Fe_3O_4 microspheres. Finally, the drug loading and release behavior under different pH environments of the resultant magnetite and tumor dual-targeting P(MBAAm-*co*-MAA) hollow microspheres were investigated with DXR as a model molecule.

The TEM micrograph of hollow P(MBAAm-*co*-MAA) microspheres was shown in Fig. 1A, which indicated that the hollow polymer microspheres had uniform morphology with an average size of 191 nm and a monodispersion of 1.016 (polydisperse index) as summarized in Table 1. The hollow-sphere structures were clearly observed in Fig. 1A with the presence of circular rings of sectional spheres and a cavity on the interior, which demonstrated that the P(MBAAm-*co*-MAA) shell-layer with thickness of 24 nm was thick and strong enough to support the resultant voids during the selective removal of PMAA cores by dissolution in ethanol. The whole synthetic procedure and the pH-sensitivity of these hollow P (MBAAm-*co*-MAA) microspheres were reported in detail by our previous work [42].

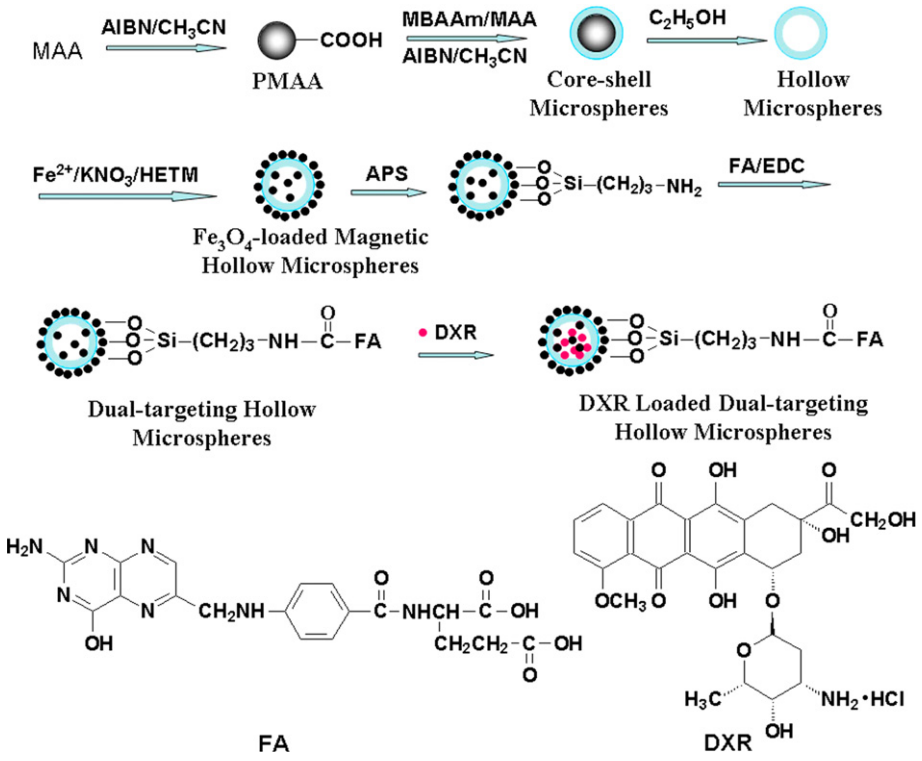

Scheme 1. Preparation of the magnetite and tumor dual-targeting P(MBAAm-*co*-MAA) hollow microspheres as anticancer drug-carriers and the chemical structures of FA and DXR molecules.

3.1. Preparation of magnetic hollow P(MBAAm-co-MAA)@Fe_3O_4 microspheres

Hollow P(MBAAm-*co*-MAA) microspheres were loaded with Fe_3O_4 nanoparticles via chemical deposition method. Iron (II) cations were captured by the carboxylate groups on the surface of hollow P(MBAAm-*co*-MAA) microspheres through coordination-interaction and some of them were inevitably permeated into hollow P(MBAAm-*co*-MAA) microspheres. In such a way, the magnetite nanoparticles were precipitated from the solution onto the hollow P(MBAAm-*co*-MAA) microspheres via the partial oxidation of ferrous (II) components with potassium nitrate as oxidant in the presence of HETM additive in EG/water solution at 80 °C.

The morphology of the Fe_3O_4 nanoparticles-loaded hollow P(MBAAm-*co*-MAA) microspheres was observed by TEM microscopy as shown in Fig. 1B, which indicated that the compact Fe_3O_4 nanoparticles (deeper contrast) with the diameters ranging from 20 to 40 nm were distributed uniformly on the surface and inside the hollow P(MBAAm-*co*-MAA) microspheres. The Fe_3O_4 nanoparticles inside the hollow microspheres may be formed via the *in-situ* precipitation of Fe_3O_4 nanoparticles after the iron cations (II) were permeated over the P(MBAAm-*co*-MAA) shell-layer into the cavity of the hollow microspheres during the partial oxidation deposition with potassium nitrate as oxidant. The average size of the magnetic P(MBAAm-*co*-MAA)@Fe_3O_4 hollow microspheres determined by DLS were 451 nm, which were bigger than the data (about 200 nm) from TEM observation. This may be due to the DLS measurement performed in aqueous solution and the magnetic P(MBAAm-*co*-MAA)@Fe_3O_4 hollow microspheres were in a swollen state. The size distribution of the magnetic hollow microspheres was shown in Fig. 1C.

Fig. 2 showed the FT-IR spectra of PMAA, PMAA/P(MBAAm-*co*-MAA) core-shell microspheres, P(MBAAm-*co*-MAA) hollow

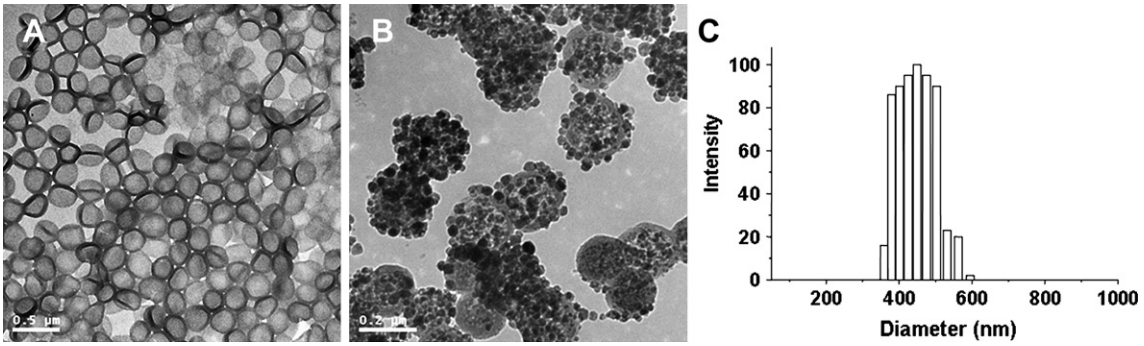

Fig. 1. TEM images of hollow P(MBAAm-*co*-MAA) microspheres (A); magnetic hollow P(MBAAm-*co*-MAA)@Fe_3O_4 microspheres (B) and the size distribution of magnetic hollow P(MBAAm-*co*-MAA)@Fe_3O_4 microspheres in ethanol by DLS (C).

Table 1
Size and size distribution of P(MBAAm-*co*-MAA) hollow microspheres.

	D_n (nm)	D_w (nm)	U[a]	Shell thickness (nm)[b]
P(MBAAm-*co*-MAA)	191	194	1.016	24

[a] Size distribution (U) = D_w/D_n.
[b] Shell thickness=($D_{P(MBAAm\text{-}co\text{-}MAA)} - D_{PMAA}$)/2.

microspheres, magnetic hollow P(EGDMA-*co*-MAA)@Fe_3O_4 microspheres. In addition to the peak at 1706 cm^{-1} corresponding to the characteristic stretching vibration of the carbonyl unit of PAA segments in Fig. 2a, the FT-IR spectrum in Fig. 2b of PMAA/P(MBAAm-*co*-MAA) core-shell microspheres had a new peak at 1524 cm^{-1} assigning to the vibration of the amide group of PMBAAm segments, proving the formation of the P(MBAAm-*co*-MAA) shell-layer during the second-stage distillation precipitation polymerization. The considerable decrease of the peak at 1708 cm^{-1} attributing to the carbonyl unit of the carboxylic acid group of PMAA segments in FT-IR spectrum of hollow P(MBAAm-*co*-MAA) microspheres in Fig. 2c and the presence of the strong wide peak at 3424 cm^{-1} assigning to the characteristic vibration of *N—H* unit and the stronger peak at 1529 cm^{-1} due to the successful removal of the PMAA cores by dissolution in ethanol. The characteristic peak corresponding to the stretching vibration of Fe—O bond was shifted to a higher wave-number of 590 cm^{-1} in Fig. 2d comparing to the peak at 570 cm^{-1} for the stretching mode of Fe—O of bulk Fe_3O_4 components reported in the literature [43,44], suggesting that Fe_3O_4 nanoparticles were bound to the carboxylate anion ($-COO^-$) on the hollow P(MBAAm-*co*-MAA) microspheres. Such results also confirmed further the formation of Fe_3O_4 nanoparticles via the precipitation of the magnetite by partial oxidation of ferrous salt with potassium nitrate as oxidant with the aid of HETM additive, which was much similar to the results reported in the literature [45].

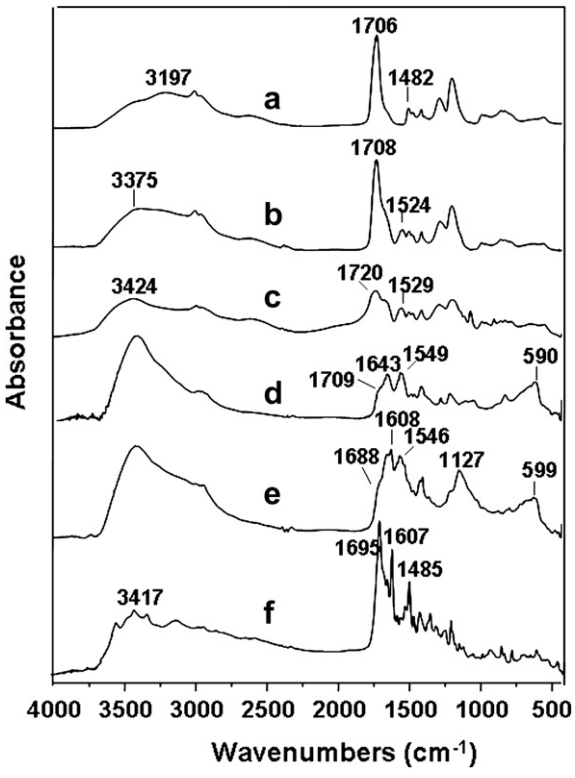

Fig. 2. FT-IR spectra: a) PMAA core; b) PMAA/P(MBAAm-*co*-MAA) core-shell microspheres; c) Hollow P(MBAAm-*co*-MAA) microspheres; d) Hollow P(MBAAm-*co*-MAA)@Fe_3O_4 microspheres; e) Magnetite and tumor dual-targeting hollow P(MBAAm-*co*-MAA) microspheres; f) FA.

The presence of magnetite on the hollow P(MBAAm-*co*-MAA)@Fe_3O_4 microspheres was proven by a superconducting quantum interference device magnetometer. The magnetization curve of hollow P(MBAAm-*co*-MAA) microspheres was measured at room temperature as shown in Fig. 3. The magnetite remanence was *S*-like curve, while the saturation magnetization of the sample was 32.52 emu g^{-1} and the magnetic remanence was 5.562 emu g^{-1}, respectively. These results indicated that Fe_3O_4 nanoparticles-loaded P(MBAAm-*co*-MAA) hollow microspheres exhibited weak ferromagnetic behavior with slender hysteresis. These magnetic hollow P(MBAAm-*co*-MAA)@Fe_3O_4 microspheres could be easily captured by a magnet as shown by the inserted photograph in Fig. 3.

3.2. Preparation of magnetite and tumor dual-targeting hollow P(MBAAm-co-MAA) microspheres

The Fe_3O_4 nanoparticles-loaded hollow P(MBAAm-*co*-MAA) microspheres having active hydroxyl groups permitted the further modification of the surface with APS possibly via the inter-condensation reaction between these active hydroxyl groups of magnetite and silanols during the sol—gel hydrolysis process as illustrated in Scheme 1, which was much similar to the modification of the surface of hematite with 3-(methacryloxy)propyl trimethoxysilane (MPS) for the preparation of hematite/polymer core-shell ellipsoids in our previous work [46]. In such a way, amino groups ($-NH_2$) were introduced onto the surface of magnetic hollow P(MBAAm-*co*-MAA)@Fe_3O_4 microspheres, which could be conjugated with FA via the amide linkages between these amino groups and the carboxylic acid groups of FA.

The FT-IR spectrum of the magnetite and tumor dual-targeting hollow P(MBAAm-*co*-MAA) microspheres via the conjugation of FA was presented in Fig. 2e. The characteristic peak of FA at 1608 and 1688 cm^{-1} were clearly observed in Fig. 2e, which were slightly shifted from the peaks of 1607 and 1695 cm^{-1} comparing to the FT-IR spectrum of folic acid in Fig. 2f. This implied that folic acid was successfully conjugated onto the magnetic hollow P(MBAAm-*co*-MAA)@Fe_3O_4 microspheres via the amide linkage between carboxylic acid groups of FA and the amino groups of the APS-modified hollow P(MBAAm-*co*-MAA)@Fe_3O_4 microspheres to

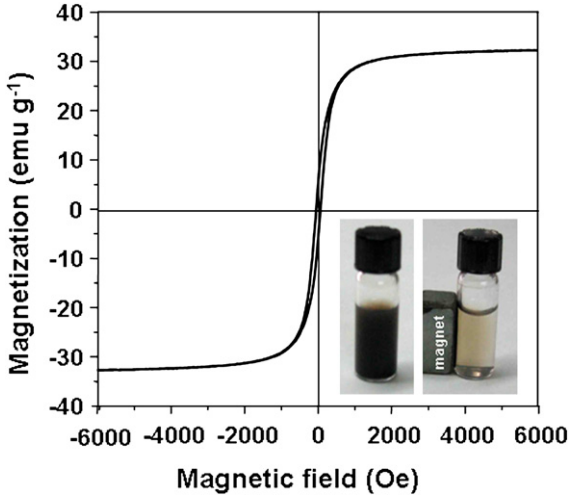

Fig. 3. Magnetization curve of hollow P(MBAAm-*co*-MAA)@Fe_3O_4 microspheres. The inset shows the photographs of the attraction of these magnetic hollow polymer microspheres dispersed in water by a magnet.

afford magnetite and tumor dual-targeting hollow polymer microspheres.

3.3. Loading and releasing behavior of DXR on magnetite and tumor dual-targeting hollow P(MBAAm-co-MAA) microspheres

To evaluate the potential application of magnetite and tumor dual-targeting hollow P(MBAAm-*co*-MAA) microspheres as a drug carrier, DXR was used as the model molecule to perform the loading and releasing test as illustrated in Scheme 1.

The magnetite and tumor dual-targeting hollow P(MBAAm-*co*-MAA) microspheres before and after loading with DXR were investigated by UV–vis absorption spectra as shown in Fig. 4. The UV–vis spectrum in Fig. 4c of the dual-targeting hollow P(MBAAm-*co*-MAA) microspheres had a strong peak at 285 nm attributing to the characteristic absorption of folic acid, was the UV–vis spectrum of folic acid in Fig. 4a had a strong peak at 283 nm. The slight shift from 283 to 285 nm in UV–vis absorption for FA species before and after the FA conjugating with dual-targeting hollow P(MBAAm-*co*-MAA)@Fe_3O_4 microspheres may be due to the formation of an amide linkage between the carboxylic acid group of FA and amino group of APS-modified hollow P(MBAAm-*co*-MAA)@Fe_3O_4 microspheres. After the magnetite and tumor dual-targeting hollow P(MBAAm-*co*-MAA) microspheres were loaded with DXR, the UV–vis peaks at around 234 and 497 nm attributing to the loaded DXR molecules were observed by the UV–vis spectrum in Fig. 4d, which were slightly shifted from the corresponding absorption peaks of free DXR molecules at 233 and 481 nm in Fig. 4e, respectively. The slight shifts of the UV–vis spectra for loaded DXR components and the conjugated FA components from 285 nm in Figs. 4c to 295 nm in Fig. 4d may be originated from the interaction of the loaded DXR drugs and the conjugated FA components. All these results demonstrated that DXR molecules were successfully loaded onto the magnetite and tumor dual-targeting hollow P(MBAAm-*co*-MAA) microspheres via the efficient interaction between the drug molecules and hollow polymer drug-carriers.

The DXR loading capacity and the encapsulation efficiency of the magnetite and tumor dual-targeting hollow P(MBAAm-*co*-MAA) microspheres were calculated according to the following formula:

$$\text{Drug loading capacity} = (W_{\text{administered dose}} - W_{\text{residual dose in solution}})/W_{\text{hollow microspheres}}$$

$$\text{Encapsulation efficiency} = (W_{\text{administered dose}} - W_{\text{residual dose in solution}})/W_{\text{administered dose}} \times 100\%$$

where $W_{\text{administered dose}}$ is the weight of drug for loading, $W_{\text{residual dose in solution}}$ is the weight of residual drug in solution after loading onto hollow polymer microspheres, and $W_{\text{hollow microspheres}}$ is the weight of hollow polymer microspheres for loading, respectively.

The loading capacity and encapsulation efficiency of DXR incorporated onto the magnetite and tumor dual-targeting hollow P(MBAAm-*co*-MAA) microspheres were investigated under different initial DXR concentrations with respect of the same concentration of dual-targeting hollow polymer microspheres (0.40 mg/mL) via the analysis of the residual DXR concentration remaining in the solution after the loading process. The results in Fig. 5 revealed that the loading capacity of the DXR on the magnetite and tumor dual-targeting hollow P(MBAAm-*co*-MAA) microspheres was increased significantly with enhancing the initial DXR concentration, then leveled off with the initial DXR concentration higher than 250 μg/mL, and saturated at the initial DXR concentration of 300 μg/mL. On the other hand, the encapsulation efficiencies of DXR were considerably decreased in the case of the initial concentrations higher than 125 μg/mL. In the present work, the initial concentration of DXR around at 230 μg/mL was considered as an appropriate value for loading process as the loading capacity (176 μg/mg) and encapsulation efficiency (61%) were comparatively high in this case.

The controlled-drug release behavior of the DXR-loaded onto the magnetite and tumor dual-targeting hollow P(MBAAm-*co*-MAA) microspheres was investigated under different pH environments with the same initial loading capacity of 176 μg/mg as shown in Fig. 6. The DXR released very slowly from the dual-targeting hollow P(MBAAm-*co*-MAA) microspheres and the releasing rate leveled off after 8 h near neutral condition (pH = 7.4). In this case, only about 28% of the loaded DXR was released from dual-targeting hollow P(MBAAm-*co*-MAA) microspheres even after 10 h 42%, 48% and 95% of the whole loaded DXR drugs on the dual-targeting hollow P(MBAAm-*co*-MAA) microspheres were released at pH of 6.0, 5.0 and 4.0 after 10 h, respectively, which were considerably faster than the releasing rate under neutral conditions as illustrated in Fig. 6. The significant dependence of the releasing behavior of

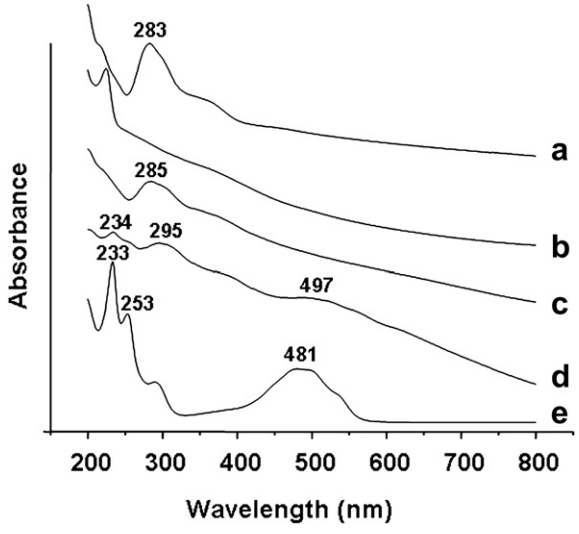

Fig. 4. UV–vis spectra: a) Free FA molecules; b) Hollow P(MBAAm-*co*-MAA)@Fe_3O_4 microspheres; c) Magnetite and tumor dual-targeting hollow P(MBAAm-*co*-MAA) microspheres; d) DXR-loaded magnetite and tumor dual-targeting hollow P(MBAAm-*co*-MAA) microspheres; e) DXR molecules.

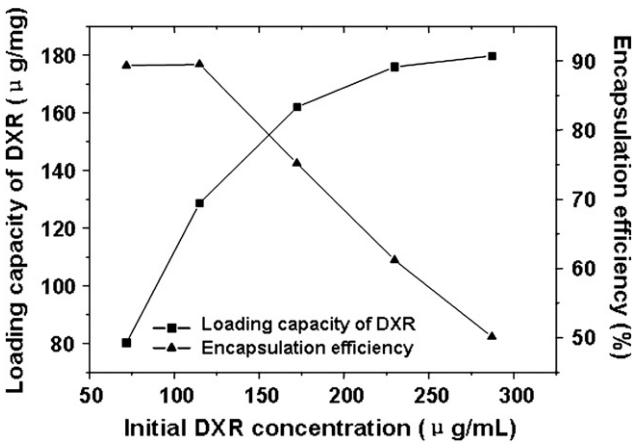

Fig. 5. The effects of initial DXR concentrations on the drug loading capacity and encapsulation efficiency of magnetite and tumor dual-targeting hollow P(MBAAm-*co*-MAA) microspheres.

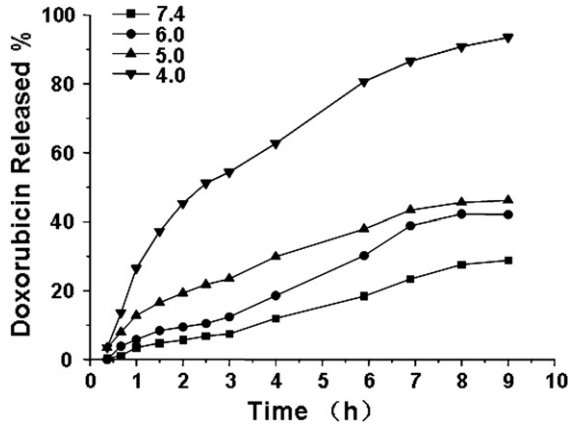

Fig. 6. The pH-dependent release behavior of loaded DXR onto magnetite and tumor dual-targeting hollow P(MBAAm-*co*-MAA) microspheres.

DXR drugs from the magnetite and tumor dual-targeting P (MBAAm-*co*-MAA) microspheres on pH values in the environment may be originated from the difference of the strength for the hydrogen-bonding interaction between the host P(MBAAm-*co*-MAA) hollow microspheres and the guest DXR molecules as well as the different swollen state of P(MBAAm-*co*-MAA) network of the hollow polymer microspheres under different pH conditions, which were much similar to the loading and releasing behavior of DXR drug with pH-responsive P(MBAAm-*co*-MAA) microspheres in our previous work [42].

4. Conclusion

The magnetite and tumor dual-targeting hollow P(MBAAm-*co*-MAA) microspheres with diameter of 191 nm and polymer shell thickness of 24 nm were prepared by deposition of Fe_3O_4 nanoparticles onto the hollow P(MBAAm-*co*-MAA) microspheres via the partial oxidation of ferrous salt in the presence of potassium nitrate as oxidant with the aid of HETM additive and the subsequent conjugation of FA through the amide linkages between the carboxylic acid groups of FA and the amino groups of APS-modified magnetic P(MBAAm-*co*-MAA)@Fe_3O_4 hollow microspheres. The hollow P(MBAAm-*co*-MAA) microspheres having the magnetite and tumor dual-targeting properties with uniform size and good morphology were confirmed by the results from TEM, FT-IR spectra, UV–vis spectra and magnetization curve. The saturation magnetization and the magnetic remanence of the dual-targeting hollow P (MBAAm-*co*-MAA) microspheres were 32.52 and 5.562 emu g^{-1}, respectively. The drug loading of the dual-targeting hollow P (MBAAm-*co*-MAA) microspheres toward DXR drug possessed good loading capacity (as high as 176 μg/mg) and high encapsulation efficiency (as high as 61%) in the case of initial DXR concentration at 230 μg/mL, while the releasing behavior with dual-targeting hollow microspheres as reservoirs was highly dependent on the pH values in the environment. All these results may offer a suitable way for the preparation of the multi-functionalized drug-carriers for tumor combination therapy.

Acknowledgement

This work was supported by the National Natural Science Foundation of China with contract No.: 20874049.

References

[1] Zhang J, Xu S, Kumacheva E. J Am Chem Soc 2004;126:7908.
[2] Cochran JK. Curr Opin Solid State Mater Sci 1998;3:474.
[3] Caruso F. Adv Mater 2001;13:11.
[4] Gill I, Ballesteros A. J Am Chem Soc 1998;120:8587.
[5] Xu XL, Asher SA. J Am Chem Soc 2004;126:7940.
[6] Pavlyuchenko VN, Sorchirskaya OV, Ivanchev SS, Klubin VV, Kreichman GS, Budtov VP, et al. J Polym Sci Polym Chem 2001;39:1090.
[7] Zha LS, Zhang Y, Yang WL, Fu SK. Adv Mater 2002;14:1090.
[8] Mandal TK, Fleming MS, Walt DR. Chem Mater 2000;12:3481.
[9] Li GL, Liu G, Kang ET, Neoh KG, Yang XL. Langmuir 2008;24:9050.
[10] Lee ES, Na K, Bae YH. J Contr Release 2005;103:405.
[11] Leroux JC, Roux E, Garree DL, Hong K, Drummond PC. J Contr Release 2001;72:71.
[12] Gao HF, Yang WL, Min K, Zha LS, Wang CC, Fu SK. Polymer 2005;46:1087.
[13] Li GL, Yang XY, Wang B, Wang JY, Yang XL. Polymer 2008;49:3436.
[14] Ibraz G, Dahen L, Donath E, Möhwald H. Adv Mater 2001;13:1324.
[15] Huang JS, Wan JR, Guo M, Yan HS. J Mater Chem 2006;16:4535.
[16] Ju XJ, Liu L, Xie R, Niu CH, Chu LY. Polymer 2009;50:922.
[17] Gu H, Ho PL, Tsang KWT, Wang L, Xu B. J Am Chem Soc 2003;125:15702.
[18] Nam JM, Thaxton CS, Hirkin CA. Science 2003;301:1884.
[19] Gupta AK, Gupta M. Biomaterials 2005;26:3995.
[20] Berry CC. J Mater Chem 2005;15:543.
[21] Lu AH, Schmidt W, Matsussevitch N, Bönnemann Hm, Spiethoff B, Teschen B, et al. Angew Chem Int Ed 2004;43:4303.
[22] Rana S, White P, Bradley M. Tetrahedron Lett 1999;40:8137.
[23] Liu XQ, Guan YP, Ma ZY, Liu HZ. Langmuir 2004;20:10278.
[24] Chen JP, Su DR. Biotechnol Prog 2001;17:369.
[25] Kawashita M, Tanaka M, Kokubo T, Inoue Y, Yao T, Hamada S, et al. Biomaterials 2005;26:2231.
[26] Deng YH, Wang CC, Shen XZ, Yang WL, Jin L, Gao H, et al. Chem Eur J 2005;11:6006.
[27] Xulu PM, Filipsel G, Zrinyi M. Macromolecules 2000;33:1716.
[28] Jones F, Colfen H, Antonietti M. Colloid Polym Sci 2000;278:491.
[29] Ugelstad J, Söderberg L, Berge A, Bergström J. Nature 1983;303:95.
[30] Lee Y, Rho J, Jung B. J Appl Polym Sci 2003;89:2058.
[31] Drescp PA, Zaotesev VS, Gambino RJ, Chu B. Langmuir 1999;15:1945.
[32] Landfester K. Adv Mater 2001;13:765.
[33] Horak D, Semanyuk N, Lednicky F. J Polym Sci Polym Chem 2003;41:1848.
[34] Laitsev VS, Filimonov DS, Presnyakov IA, Gambino RJ, Chu B. J Colloid Interface Sci 1999;212:49.
[35] Vestal CR, Zhang ZJ. J Am Chem Soc 2002;124:14312.
[36] Liu QX, Xu ZH, Finch JA, Egerton R. Chem Mater 1998;10:3936.
[37] Low PS, Kularatne SA. Curr Opin Chem Biol 2009;13:256.
[38] Ratnam M, Hao H, Zheng X, Wang H, Qi H, Lee R, et al. Expet Opin Biol Ther 2003;3:563.
[39] Kelley KM, Rowan BG, Ratnam M. Cancer Res 2003;63:2820.
[40] Duncan R. Anti Canc Drugs 1992;3:175.
[41] Bae Y, Fukushima S, Harada A, Kataoka K. Angew Chem Int Ed 2003;42:4640.
[42] Yang XY, Chen LT, Huang B, Bai F, Yang XL. Polymer 2009;50:3556.
[43] Chin SF, Iyer KS, Raston CL. Lab on a Chip 2008;8:439.
[44] Rocchiccioli-Deltche C, Franck R, Cabuil V, Massart R. J Chem Res 1987;5:126.
[45] Huang ZB, Tang FQ. J Colloid Interface Sci 2005;281:432.
[46] Liu GY, Li LY, Yang XL. Polymer 2008;49:4776.